Engineering Analysis with Boundary Elements 37 (2013) 15–22

Contents lists available at SciVerse ScienceDirect

Engineering Analysis with Boundary Elements

journal homepage: www.elsevier.com/locate/enganabound

Three-dimensional transient heat conduction analysis by Laplace transformation and multiple reciprocity boundary face method

Shuaiping Guo, Jianming Zhang*, Guangyao Li, Fenglin Zhou

State Key Laboratory of Advanced Design and Manufacturing for Vehicle Body, College of Mechanical and Vehicle Engineering, Hunan University, Changsha 410082, China

ARTICLE INFO

Article history:
Received 7 May 2012
Accepted 1 September 2012

Keywords:
Transient heat conduction
Boundary integral equations
Boundary face method
Laplace transformation
Multiple reciprocity method

ABSTRACT

In this paper, a new multiple reciprocity formulation is developed to solve the transient heat conduction problem. The time dependence of the problem is removed temporarily from the equations by the Laplace transform. The new formulation is derived from the modified Helmholtz equation in Laplace space (LS), in which the higher order fundamental solutions of this equation are firstly derived and used in multiple reciprocity method (MRM). Using the new formulation, the domain integrals can be converted into boundary integrals and several non-integral terms. Thus the main advantage of the boundary integral equations (BIE) method, avoiding the domain discretization, is fully preserved. The convergence speed of these higher order fundamental solutions is high, thus the infinite series of boundary integrals can be truncated by a small number of terms. To get accurate results in the real space with better efficiency, the Gaver-Wynn-Rho method is employed. And to integrate the geometrical modeling and the thermal analysis into a uniform platform, our method is implemented based on the framework of the boundary face method (BFM). Numerical examples show that our method is very efficient for transient heat conduction computation. The obtained results are accurate at both internal and boundary points. Our method outperforms most existing methods, especially concerning the results at early time steps.

1. Introduction

Transient heat conduction problems can be efficiently solved by the boundary integral equation method [1]. The various solution procedures reported in the literature can essentially be classified into two broad categories: the time domain approach and the transform space approach [1–3]. The first boundary integral solution for the diffusion equation was proposed by Rizzo and Shippy [2]. In their approach, the time dependence of the problem is temporarily removed with the Laplace transform. Using the transform, the parabolic heat conduction equation is transformed into a more tractable elliptic equation. Then the boundary integral equation is derived and solved in the Laplace space for a sequence of real positive values of the transform parameter. Finally, the inverse transformation is performed to evaluate the physical variables in the real space. Chang et al. [3] employed time-dependent fundamental solutions in the context of the direct method to solve two-dimensional problems of heat conduction in isotropic and anisotropic media in 1973. The both categories of approaches suffer from the time-consuming domain integral calculation.

The unsteady heat conduction problem without heat source and non-uniform initial temperature distribution can be easily solved by the conventional boundary element method (BEM) without using internal cells. For special cases, unsteady heat conduction problems with constant heat generation and uniform initial temperature distribution can also be solved by the conventional BEM [4]. However, the domain integral is necessary in the cases where the initial temperature distribution is not uniform and the heat generation function is arbitrary. In these cases, the basic advantage of dimensionality reduction is lost in the BEM. To avoid the domain integration, several methods have been proposed. Tanaka et al. [5] introduced the dual reciprocity method (DRM) to solve the diffusion problem. In that method, a number of internal points for approximation of the non-homogeneous term are necessary. Nowak and Neves [6,7] applied the multiple reciprocity method (MRM) to convert the domain integral to an infinite series of boundary integrals using the higher-order fundamental solutions. In Reference [6], the authors tried to solve the transient problems with the fundamental solution and higher order fundamental solutions of the Laplace equation. In the MRM, however, numerical instability was found when the length of time step is small. Moreover, the higher order derivatives of the time-dependent fundamental solutions are complicated and the verification of the convergence has not been found in existing literatures. Nevertheless, applications of the

* Corresponding author. Tel.: +86 731 88823061.
E-mail address: zhangjianm@gmail.com (J. Zhang).

0955-7997/$ - see front matter © 2012 Elsevier Ltd. All rights reserved.
http://dx.doi.org/10.1016/j.enganabound.2012.09.001

MRM have been found. Chen and Wong [8] extended the dual formulation for the MRM to solve the acoustic modes successfully. A series-type complex-valued dual BEM call the complete MRM was derived in [9]. Based on the MRM, Ochiai and Kitayama [4] proposed a triple reciprocity method. In some cases, however, this method still applies internal points for variable interpolation.

In this paper, the Laplace transformation technology was applied to eliminate the time-dependence. In LS, we can get the weighted residual statement of the control equation with the fundamental solution. Furthermore, the fundamental solution is derived from the modified Helmholtz equation rather than the Laplace equation. The MRM is applied to avoid the domain integration related to the initial distribution and heat generations. By using MRM, the domain integral is converted to an infinite series of boundary integrals. These infinite series are truncated for practical implementations. The higher order forms of the fundamental solution used in MRM are first derived using a reciprocity scheme. These forms of the fundamental solution are simpler than conventional formulations used in Ref. [6]. In addition, these higher order forms are only constant times of the original fundamental solution. Thus the formulation of MRM is of simple form.

To avoid the differences between the geometric model and the analysis model, Zhang proposed the boundary face method (BFM) in [10,11]. In the BFM, the boundary integration is performed on boundary faces, which are represented in parametric form and directly derived from the boundary representation data structure in solid modeling. The integrand quantities, such as the coordinates of Gauss integration points, Jacobian and out normal are calculated directly from the faces rather than from elements. By coupling with the DRM, Zhou [12,13] extended the BFM for non-homogeneous problem. Our method is implemented in the framework of boundary face method (BFM) program.

After solving the BIE in LS, the inversion of Laplace transform is another important issue. The analytical inversion of Laplace transform is known to be ill-posed. In other words, small changes of value in Laplace space may lead to large disturbance in the real space. So the method for numerical inversion is of great importance to the accuracy of the result. There are several numerical algorithms in literature that can be used to perform the inverse Laplace transform. The most commonly known numerical inversion procedures are Fourier series method [14,15], Talbot's method [16,17], Weeks' method [18,19] and post-Gaver's method [17,20–22]. To balance the accuracy and efficiency of the computation, the Gaver-Wynn-rho algorithm, which use the Wynn's rho algorithm to improve the convergence rate of Gaver's algorithm, is applied in this paper.

2. Problem definition

2.1. Governing equation, boundary conditions and initial conditions

If the material is isotropic and there is no internal generation inside the domain, the transient potential problem can be represented as

$$\nabla^2 u(x,t) = \frac{1}{a}\frac{\partial u(x,t)}{\partial t} \quad x \in \Omega \tag{1}$$

where $u(x,t)$ is the temperature of the location x at the time t. The coefficient a is the thermal diffusivity. Ω stands for the considered domain enclosed by $\Gamma_1 \cup \Gamma_2$, the boundary conditions are given as the following types

$$\begin{aligned} &u(x,t) = \overline{u}(x,t), && x \in \Gamma_1 \\ &q(x,t) = \tfrac{\partial u(x,t)}{\partial n(x)} = \overline{q}(x,t), && x \in \Gamma_2 \end{aligned} \tag{2}$$

in which $\overline{u},\overline{q}$ stand for the prescribed temperature and normal flux on the boundary. Initial conditions at time $t=t_0$ can be prescribed

$$u_0(x) = u(x,t_0). \quad x \in \Omega \tag{3}$$

We denote the Laplace transform of a function $u(x,t)$ by

$$\tilde{u}(x,s) = L(u(x,t)) = \int_0^\infty u(x,t)e^{-st}dt \tag{4}$$

And we assume the transform parameter s is real and positive. After integration by parts, we can obtain

$$L\left(\frac{\partial u(x,t)}{\partial t}\right) = s\tilde{u}(x,s) - u_0(x) \tag{5}$$

Implementing the Laplace transform on Eq. (1), we have the following governing equation.

$$\nabla^2 \tilde{u}(x,s) - \frac{s}{a}\tilde{u}(x,s) + \frac{1}{a}u_0(x) = 0 \tag{6}$$

It is worth noting that this is actually a modified Helmholtz equation. With the same transform, the boundary condition for Eq. (6) is

$$\begin{aligned} &\tilde{u}(x,s) = \overline{u}(x,s). && x \in \Gamma_1 \\ &\tilde{q}(x,s) = \overline{q}(x,s). && x \in \Gamma_2 \end{aligned} \tag{7}$$

2.2. A new form fundamental solution and its MRM formulation

We denote u^* for the fundamental solution of Eq. (6), and it satisfies the following equation

$$\nabla^2 u^*(x,s) - \lambda u^*(x,s) = \Delta(x,\xi) \tag{8}$$

In Ref. [1], the fundamental solution for the above equation is

$$u^* = \frac{-\lambda^{1/4}}{r^{1/2}(2\pi)^{3/2}}K_{1/2}\left[\lambda^{1/2}r\right] \tag{9}$$

where $\lambda = s/a$ and K_ν is the modified Bessel function of the second kind of order ν [1]. Substituting the following equation to Eq. (9)

$$K_{1/2}[x] = \sqrt{\frac{\pi}{2x}}e^{-x} \tag{10}$$

we have a simple form of the above fundamental solution.

$$u^* = \frac{-1}{4\pi r}e^{-\sqrt{\lambda}r} \tag{11}$$

The derivative of the fundamental solution is rewritten as

$$q^* = \frac{\partial u^*}{\partial n} = \frac{1}{4\pi r^2}(1+\sqrt{\lambda}r)e^{-\sqrt{\lambda}r} \times \frac{\partial r}{\partial n} \tag{12}$$

By employing the fundamental solution in Eq. (11) and Eq. (12), Eq. (6) can be converted into the following BIE:

$$\int_\Gamma q^* \times \tilde{u}\,d\Gamma - c \times \tilde{u}(Y) - \int_\Gamma u^* \times \tilde{q}\,d\Gamma = \frac{1}{a}\int_\Omega u^* \times u_0\,d\Omega \tag{13}$$

In Eq. (13), the value of the constant c is

$$c = \begin{cases} 0 & Y \in \overline{\Omega} \\ 1 & Y \in \Omega \\ 0.5 & Y \in \Gamma_1 \cup \Gamma_2 \end{cases} \tag{14}$$

The higher order fundamentals are necessary when using the MRM in conversion of the domain integral. A sequence of higher order fundamental solutions can be defined by the recurrence formula:

$$
\begin{aligned}
&u^{*(0)} = u^* \\
&\nabla^2 u^{*(j+1)} = u^{*(j)} \quad j = 0,1,2,\ldots \\
&q^{*(j+1)} = \tfrac{\partial u^{*(j+1)}}{\partial n}
\end{aligned}
\tag{15}
$$

or by the formula:

$$
\begin{aligned}
u^{*(j)} &= (1/\lambda^j) u^{*(0)} \quad j = 0,1,2,\ldots \\
q^{*(j)} &= (1/\lambda^j) q^{*(0)}
\end{aligned}
\tag{16}
$$

From Eq. (16), it is found that the higher order solutions are obtained from their corresponding original fundamental solution by multiplying a constant term. It is much more convenient than the conventional higher order solutions. Furthermore, the influence matrices which arise from the higher order forms are just the times of that arise from the fundamental solutions, the storage of the all matrices can be vastly reduced by only keeping the matrices from the fundamental solution.

In the conventional MRM, the $u^{*(j)}$ in domain integrals are replaced by $\nabla^2 u^{*(j+1)}$ in the following BIE:

$$
\begin{aligned}
&\int_\Omega u^{*(j)} \times u_0^{(j)}(x) d\Omega \\
&= \int_\Omega \nabla^2 u^{*(j+1)} \times u_0^{(j)}(x) d\Omega \\
&= \int_\Omega u^{*(j+1)} \times \nabla^2 u_0^{(j)}(x) d\Omega + \int_\Gamma q^{*(j+1)} \times u_0^{(j)} d\Gamma \\
&\quad - \int_\Gamma u^{*(j+1)} \times u_0^{(j)} d\Gamma \\
&= \int_\Omega u^{*(j+1)} \times u_0^{(j+1)}(x) d\Omega + \int_\Gamma q^{*(j+1)} \times u_0^{(j)} d\Gamma \\
&\quad - \int_\Gamma u^{*(j+1)} \times u_0^{(j)} d\Gamma
\end{aligned}
\tag{17}
$$

Considering Eq. (15), we reform Eq. (8) into the following equation:

$$
u^* = (1/\lambda)\nabla^2 u^* - (1/\lambda)\Delta(x, Y) = \nabla^2 u^{*(1)} - (1/\lambda)\Delta(Y, x) \tag{18}
$$

where we still adopt the mark of $u^{*(j)}$and $q^{*(j)}$ as in Eq. (16). Thus in our method, the relationship between the fundamental solution and its higher order forms is a little different from Eq. (15). For domain integration, the second item on the right of Eq. (18) is evaluated using the function of Y. Substituting Eq. (18) into the domain integral term in Eq. (13), it yields:

$$
\begin{aligned}
\int_\Omega u^* \times u_0 d\Omega &= \int_\Omega \left(\nabla^2 u^{*(1)} - \frac{1}{\lambda} \Delta(Y, x) \right) \times u_0 d\Omega \\
&= \int_\Omega \nabla^2 u^{*(1)} \times u_0 d\Omega - c \frac{1}{\lambda} u_0(Y)
\end{aligned}
\tag{19}
$$

Then we apply the higher order fundamental solutions to substitute the lower order one in the reciprocity theorem, and the following representation should be employed:

$$
u^{*(j)} = (1/\lambda^j) u^{*(0)} = \nabla^2 u^{*(j+1)} - (1/\lambda^{j+1})\Delta(Y, x) \tag{20}
$$

In our implementation additional quantities are required. These quantities include the initial temperature, initial normal flux and their higher order forms, which are listed below.

$$
\begin{aligned}
&u_0^{(0)} = u_0 \quad u_0^{(j)} = \nabla^2 u_0^{(j-1)} \\
&q_0 = \tfrac{\partial u_0}{\partial n} \quad q_0^{(j)} = \tfrac{\partial u_0^{(j)}}{\partial n}
\end{aligned}
\tag{21}
$$

Using reciprocity scheme, the domain integral can be represented recursively by

$$
\begin{aligned}
&\textstyle\int_\Omega u^{*(j)} \times u_0^{(j)}(x) d\Omega = \int_\Omega \left(\nabla^2 u^{*(j+1)} - \frac{1}{\lambda^{j+1}} \Delta(Y, x) \right) \times u_0^{(j)}(x) d\Omega \\
&= \int_\Omega \nabla^2 u^{*(j+1)} \times u_0^{(j)}(x) d\Omega - \frac{c}{\lambda^{j+1}} u_0^{(j)}(Y) \\
&= \int_\Omega u^{*(j+1)} \times \nabla^2 u_0^{(j)}(x) d\Omega + \int_\Gamma q^{*(j+1)} \times u_0^{(j)} d\Gamma \\
&\quad - \int_\Gamma u^{*(j+1)} \times u_0^{(j)} d\Gamma - \frac{c}{\lambda^{j+1}} u_0^{(j)}(Y) \\
&= \int_\Omega u^{*(j+1)} \times u_0^{(j+1)}(x) d\Omega + \int_\Gamma q^{*(j+1)} \times u_0^{(j)} d\Gamma \\
&\quad - \int_\Gamma u^{*(j+1)} \times u_0^{(j)} d\Gamma - \frac{c}{\lambda^{j+1}} u_0^{(j)}(Y)
\end{aligned}
\tag{22}
$$

And totally by:

$$
\begin{aligned}
\int_\Omega u^* \times u_0 d\Omega &= \sum_{j=0}^{\infty} \left(\int_\Gamma q^{*(j+1)} \times u_0{}^{(j)} d\Gamma - \int_\Gamma u^{*(j+1)} \times q_0{}^{(j)} d\Gamma \right) \\
&\quad - c \sum_{j=0}^{\infty} \frac{1}{\lambda^{j+1}} u_0^{(j)}(Y) \\
&= \int_\Gamma q^* \times \sum_{j=0}^{\infty} \frac{1}{\lambda^{j+1}} u_0{}^{(j)} d\Gamma - \int_\Gamma u^* \times \sum_{j=0}^{\infty} \frac{1}{\lambda^{j+1}} q_0{}^{(j)} d\Gamma \\
&\quad - c \sum_{j=0}^{\infty} \frac{1}{\lambda^{j+1}} u_0^{(j)}(Y)
\end{aligned}
\tag{23}
$$

If the initial temperature distribution can be expressed by a polynomial function, $u_0^{(j)}$and $q_0^{(j)}$approach to zero with an increasing j. Thus the infinite series of boundary integrals will become finite exactly. If the initial temperature distribution is more general, bearing in mind the convergence of the higher order fundamental solution, the infinite series can also be computed through several truncated terms. The convergence will be discussed in Section 2.5. Truncating the series in Eq. (23) by M terms, and then substituting it into Eq. (13), we have

$$
\begin{aligned}
&\int_\Gamma q^* \tilde{u} d\Gamma - c \times \tilde{u}(Y) - \int_\Gamma u^* \tilde{q} d\Gamma \\
&= \frac{1}{a} \int_\Gamma q^* \times \sum_{j=0}^{M-1} \frac{1}{\lambda^{j+1}} u_0{}^{(j)} d\Gamma \\
&\quad - \frac{1}{a} \int_\Gamma u^* \times \sum_{j=0}^{M-1} \frac{1}{\lambda^{j+1}} q_0{}^{(j)} d\Gamma - \frac{c}{a} \sum_{j=0}^{M-1} \frac{1}{\lambda^{j+1}} u_0^{(j)}(Y)
\end{aligned}
\tag{24}
$$

In matrix notation, approximations of potential and flux for each boundary element can be expressed by the following general system

$$
\begin{aligned}
\tilde{u}(x) &= \Phi^T \tilde{u}_n \\
\tilde{q}(x) &= \Phi^T \tilde{q}_n
\end{aligned}
\tag{25}
$$

with $\tilde{u}_n$and $\tilde{q}_n$ being the vectors referring to the nth boundary element and containing nodal values of potential and flux, respectively. The row matrix Φ^T contains the local shape functions. The number of column of this matrix depends on the type of boundary elements. Discretization of the boundary Γ into boundary elements allows one to replace the integrals in Eq. (24) by the summation of integrals, each one along particular boundary element Γ_n

$$
\begin{aligned}
&\sum_{n=1}^{N} \int_{\Gamma_n} q^* \tilde{u} d\Gamma_n - c_i \tilde{u}(Y) - \sum_{n=1}^{N} \int_{\Gamma_n} u^* \tilde{q} d\Gamma_n \\
&= \frac{1}{a} \sum_{n=1}^{N} \left(\int_{\Gamma_n} q^* \times \sum_{j=0}^{M-1} \frac{1}{\lambda^{j+1}} u_0{}^{(j)} d\Gamma_n - \int_{\Gamma_n} u^* \times \sum_{j=0}^{M-1} \frac{1}{\lambda^{j+1}} q_0{}^{(j)} d\Gamma_n \right) \\
&\quad - \frac{c}{a} \sum_{j=0}^{M-1} \frac{1}{\lambda^{j+1}} u_0^{(j)}(Y)
\end{aligned}
\tag{26}
$$

Finally, we collocate the field points at all interpolation points and the following system of linear equations is obtained

$$
HU - GQ = R \tag{27}
$$

where the entries of the matrices are

$$H=H^0-0.5I \quad G=G^0$$

$$R=\frac{1}{a}\sum_{j=0}^{M-1}(H^{j+1}U_0^j-G^{j+1}Q_0^j)=\frac{1}{a}\times H\sum_{j=0}^{M-1}\frac{1}{\lambda^{j+1}}U_0{}^{(j)}-\frac{1}{a}\times G\sum_{j=0}^{M-1}\frac{1}{\lambda^{j+1}}Q_0{}^{(j)}$$

$$H_{ij}^0=\int_{\Gamma_j}\Phi^T q^* d\Gamma_j \quad H_{ij}^k=\int_{\Gamma_j}\Phi^T q^{*(k)}d\Gamma_j=\tfrac{1}{\lambda^k}H_{ij}^0$$

$$G_{ij}^0=\int_{\Gamma_j}\Phi^T u^* d\Gamma_j \quad G_{ij}^k=\int_{\Gamma_j}\Phi^T u^{*(k)}d\Gamma_j=\tfrac{1}{\lambda^k}G_{ij}^0 \tag{28}$$

where vectors $U_0^{(j)}$, $Q_0^{(j)}$ are built up from nodal values of functions $u_0^{(j)}$, $q_0^{(j)}$, respectively.

2.3. The MRM formulation with the heat generation

The transient heat conduction problem with heat generation can be represented as

$$\frac{\partial u}{\partial t}=a\nabla^2 u+\frac{1}{c\rho}f(x,t) \quad x\in\Omega \tag{29}$$

where $f(x, t)$ are the heat source density, the coefficients c and ρ are the specific heat and the density, respectively. After Laplace transform, the govern equation is

$$\nabla^2\tilde{u}-\lambda\tilde{u}=-\frac{1}{a}u_0-\frac{1}{k}\tilde{f}(x,s) \tag{30}$$

where the coefficient k is the heat conductivity. We denote for short

$$b(x,s)=\frac{1}{a}u_0+\frac{1}{k}\tilde{f}(x,s) \tag{31}$$

The BIE is:

$$\int_\Gamma q^*\tilde{u}d\Gamma-c\times\tilde{u}(Y)-\int_\Gamma u^*\tilde{q}d\Gamma=\int_\Omega u^*\times b(x,s)d\Omega \tag{32}$$

Similar to Eq. (23), the domain integral term in the right hand side of Eq. (32) can be represented by

$$\int_\Omega u^*\times b(x,s)d\Omega=\int_\Gamma q^*\times\sum_{j=0}^{\infty}\frac{1}{\lambda^{j+1}}b^{(j)}d\Gamma-\int_\Gamma u^*\times\sum_{j=0}^{\infty}\frac{1}{\lambda^{j+1}}b_n{}^{(j)}d\Gamma-\frac{1}{2}\sum_{j=0}^{\infty}\frac{1}{\lambda^{j+1}}b^{(j)}(Y) \tag{33}$$

The higher order source functions are expressed as

$$\begin{aligned}
&\tilde{f}^{(0)}(x,s)=\tilde{f}(x,s)\\
&\tilde{f}^{(j)}(x,s)=\nabla^2\tilde{f}^{(j-1)}(x,s)\\
&b^{(0)}(x,s)=\tfrac{1}{a}u_0+\tfrac{1}{k}\tilde{f}^{(0)}(x,s)\\
&b^{(j)}=\tfrac{1}{a}u_0^{(j)}(x,s)+\tfrac{1}{k}\tilde{f}^{(j)}(x,s)\\
&b_n^{(j)}=\tfrac{\partial b^{(j)}}{\partial n}=\tfrac{1}{a}\tfrac{\partial u_0^{(j)}(x)}{\partial n}+\tfrac{1}{k}\tfrac{\partial\tilde{f}^{(j)}(x,s)}{\partial n}
\end{aligned} \tag{34}$$

We can truncate the series appropriately in Eq. (33) by M terms

$$\int_\Gamma q^*\tilde{u}d\Gamma-\frac{1}{2}\tilde{u}(Y)-\int_\Gamma u^*\tilde{q}d\Gamma=\sum_{j=0}^{M-1}\left(\int_\Gamma\tilde{q}^{*(j+1)}\times b^{(j)}d\Gamma-\int_\Gamma\tilde{u}^{*(j+1)}\times b_n^{(j)}d\Gamma\right)-\sum_{j=0}^{M-1}\frac{1}{\lambda^{j+1}}b^{(j)}(Y) \tag{35}$$

Eq. (35) can be expressed by matrix form as

$$H=H^0-0.5I \quad G=G^0$$

$$F=\sum_{j=0}^{M-1}(H^{j+1}B^j-G^{j+1}B_n^j)=H\sum_{j=0}^{M-1}\frac{1}{\lambda^{j+1}}B^j-G\sum_{j=0}^{M-1}\frac{1}{\lambda^{j+1}}B_n^j \tag{36}$$

where the matrix I is the identity matrix.

2.4. The derivation of the fundamental solution

For the field point $Y\in\Omega$, the integral equation is:

$$\tilde{u}(Y)=\int_\Gamma q^*\tilde{u}d\Gamma-\int_\Gamma u^*\tilde{q}d\Gamma-\int_\Omega u^*\times b(x,s)d\Omega \tag{37}$$

After substitution of Eq. (33) into Eq. (37), the equation becomes

$$\tilde{u}(Y)=\int_\Gamma q^*\left(\tilde{u}-\sum_{j=0}^{M-1}\frac{1}{\lambda^{j+1}}b^{(j)}\right)d\Gamma-\int_\Gamma u^*\left(\tilde{q}-\sum_{j=0}^{M-1}\frac{1}{\lambda^{j+1}}b_n^{(j)}\right)d\Gamma+\sum_{j=0}^{M-1}\frac{1}{\lambda^{j+1}}b^{(j)}(Y) \tag{38}$$

To compute the flux inside the domain, furthermore, the following hyper-singular BIE is applied.

$$\frac{\partial\tilde{u}(Y)}{\partial x_i}=\int_\Gamma\frac{\partial q^*}{\partial x_i}\left(\tilde{u}-\sum_{j=0}^{N-1}\frac{1}{\lambda^{j+1}}b^{(j)}\right)d\Gamma-\int_\Gamma\frac{\partial u^*}{\partial x_i}\left(\tilde{q}-\sum_{j=0}^{N-1}\frac{1}{\lambda^{j+1}}b_n^{(j)}\right)d\Gamma+\sum_{j=0}^{N-1}\frac{1}{\lambda^{j+1}}\frac{\partial b^{(j)}(Y)}{\partial x_i}$$

$$\tilde{q}(Y)=\sqrt{\sum_{i=1}^{3}\left(\frac{\partial\tilde{u}(Y)}{\partial x_i}\right)^2} \tag{39}$$

So the derivative of the fundamental solution is expressed as follows

$$\frac{\partial u^*}{\partial x_i}=\frac{(1+\lambda r)}{4\pi r^2}e^{-\lambda r}\frac{x_i-Y_i}{r}$$

$$\frac{\partial q^*}{\partial x_i}=\frac{e^{-\lambda r}}{4\pi r^3}\left\{\left[-3(1+\lambda r)-\lambda^2 r^2\right]dx_i\frac{\partial r}{\partial n}+(1+\lambda r)n_i\right\} \quad i=1,2,3 \tag{40}$$

where (Y_1,Y_2,Y_3) is the source point Y and $(n_1,n_2,n_3)$is the outward normal to the boundary at the point x.

2.5. The convergence of the MRM formulations

In general, the value of the series in formula (33) is affected by the numerical discretization of the boundary as well as by the number of the truncated terms in the series. It is obvious that the numerical mesh has to be appropriate to represent accurately the changes of the problem variables. However, since this is a common problem in many numerical methods, this topic will not be discussed here. We study the criteria when the series (33) converges and the way of controlling the required number of terms.

In the first case, the domain distributions including initial temperature distribution and source distribution is of constant type or polynomial type, the MRM converges naturally. It is worth noting that, in many practical cases, the considered domain distribution can be approximated by these simple distributions. In cases of these simple distributions, the domain integrals can be analytically converted to boundary integrals through several reciprocal procedures. Thus there is no convergent problem in this case.

In the second case, the MRM series for representing the domain distribution do not converge quickly or the value of the higher order functions even increase at a certain speed. In this case, the higher order fundamental solutions are of more importance to the convergence of the expansion than the higher order functions.

Table 1
Thermal diffusivity of several materials.

Materials and substances	Pyrolytic graphite, parallel to layers	Silver, pure (99.9%)	Steel, 1% carbon	Water vapour (1 atm, 400 k)	Steel, stainless 304A
Thermal diffusivity (m^2/s)	1.22×10^{-3}	1.6563×10^{-4}	1.172×10^{-5}	2.338×10^{-5}	4.2×10^{-6}

The convergence criterion can be derived from the condition that the ratio of two subsequent terms is less than 1. This can be written in terms of inequalities as follows

$$\left|\frac{u^{*(j+2)}b_n^{(j+1)}}{u^{*(j+1)}b_n^{(j)}}\right|<1 \quad \text{and} \quad \left|\frac{q^{*(j+2)}b^{(j+1)}}{q^{*(j+1)}b^{(j)}}\right|<1 \tag{41}$$

In our method, the higher order fundamental solution is of the following relation:

$$\frac{u^{*(j+2)}}{u^{*(j+1)}}=\frac{q^{*(j+2)}}{q^{*(j+1)}}=\frac{1}{\lambda} \tag{42}$$

where λ is a coefficient related with the thermal diffusivity a and the time variable t.

$$\lambda=\frac{s_n}{a}=\frac{n\times\log 2}{a\times t} \quad n=1,2,\ldots,2N \tag{43}$$

We substitute Eq. (42) and Eq. (43) into Eq. (41), the criterion becomes

$$\begin{aligned}&\left|\frac{b_n^{(j+1)}}{b_n^{(j)}}\right|<\left|\frac{u^{*(j+1)}}{u^{*(j+2)}}\right|=\min\left(\left|\frac{n\times\log2}{a\times t}\right|\right)=\left|\frac{\log2}{a\times t}\right|=\lambda_{\min}\\&\left|\frac{b^{(j+1)}}{b^{(j)}}\right|<\left|\frac{q^{*(j+1)}}{q^{*(j+2)}}\right|=\lambda_{\min}\end{aligned} \tag{44}$$

In practical materials, the value of the thermal diffusivity is usually very small. The value of $\lambda_{\min}$ will be large enough to satisfy Eq. (44). The thermal diffusivities of several materials are listed in Table 1. This can be also found in the website of Wikipedia [23].

Our method converges when domain distribution satisfies the following relations.

$$\left|\frac{b_n^{(j+1)}}{b_n^{(j)}}\right|<\lambda_{\min} \tag{45}$$

and

$$\left|\frac{b^{(j+1)}}{b^{(j)}}\right|<\lambda_{\min} \tag{46}$$

It can be seen from the convergent criterion Eq. (45) and Eq. (46) that the convergence of MRM also depends on the time variable t. For short time simulation, the value of $\lambda_{\min}$ is very big and the convergent criterion is satisfied easily. But for long time simulation, the convergent criterion is usually unsatisfied. Thus, this method is not suggested to be directly applied to simulate the transient heat conduction for a long time simulation, which is a limitation of the proposed method. In the long time simulation, however, other additional approach as approximating source distribution can be applied in the MRM to circumvent the convergent problem [4].

2.6. *Laplace inversion*

In the Laplace transform boundary integral equation method approach, the numerical inversion of the Laplace transform is very important. There are many powerful algorithms to compute the numerical inversion.

In 1941 Post–Widder provided the analytic solution of the Laplace inverse. Gaver [20] presented the discrete analog of Post–Widder formula in 1966. After expanding the difference operator, the formula can be written as

$$f_k(t)=\frac{\alpha k}{t}\binom{2k}{k}\sum_{j=0}^{k}(-1)^j\binom{k}{j}\hat f\left(\frac{(k+j)\alpha}{t}\right) \tag{47}$$

where α=log 2. The computation of it only processes in real number space and its implement is the easiest one. In this paper, the Gaver functionals is applied. The Gaver functionals can also be computed by the following recursive formulas:

$$\begin{aligned}&G_0^{(n)}=\tfrac{n\alpha}{t}\hat f(n\alpha/t), \quad 1\le n\le 2N\\&G_k^{(n)}=(1+\tfrac{n}{k})G_{k-1}^{(n)}-(\tfrac{n}{k})G_{k-1}^{(n+1)}, \quad k\ge1, n\ge k\\&f_k(t)=G_k^{(k)}\end{aligned} \tag{48}$$

Our implementation mainly consists of three steps. First of all, we should determine the value of t and N. Then $2N$ systems in Laplace space should be solved. After that, we compute $f_1(t), f_2(t),\ldots, f_{2N}(t)$ using the formulation (48).

In practical applications, the Gaver functionals usually provides a very poor approximation because $|f(t)-f_k(t)|-c/k$ as $k\to\infty$. For example, $f_{1000}(t)$ may yield an estimate to $f(t)$ with only two or three digits of accuracy. To achieve a good approximation, a convergence acceleration algorithm is required for the sequence $f_k(t)$. Valko and Abate [17,21] studied some nonlinear sequence transformations applied to the Gaver functionals and find that the Wynn's rho algorithm is the most effective one which is given by the recursive algorithm

$$\begin{aligned}&\rho_{-1}^{(n)}=0,\ \rho_0^{(n)}=f_n(t), \quad n\ge0\\&\rho_k^{(n)}=\rho_{k-2}^{(n+1)}+\frac{k}{\rho_{k-1}^{(n+1)}-\rho_{k-1}^{(n)}}. \quad k\ge1\end{aligned} \tag{49}$$

Then the approximation to $f(t)$ is obtained as

$$f_k(t,N)=\rho_N^{(0)} \tag{50}$$

The integer N must be even. As N increases the accuracy of the approximant $f(t,N)$ also increases. Using Wynn's rho algorithm the relative error estimate

$$\left|\frac{f(t)-f(t,N)}{f(t)}\right|\approx10^{-0.8N} \tag{51}$$

That is, number of significant digits in the approximant $f(t,N)$ is about N.

3. Numerical examples

To verify the efficiency of our method, solutions for three transient heat conduction problems with different type of condition and with different geometries are presented in this section.

Example 1. A suddenly heated cube

In the first example, we consider a unit cube with no initial temperature. As presented in Ref. [24], the cube is suddenly heated on the top face such that a temperature of 100 °C is

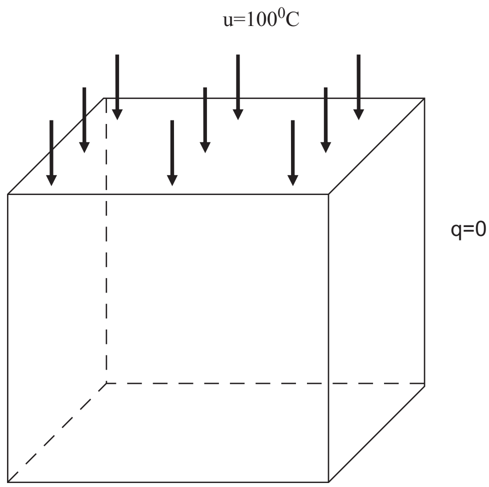

Fig. 1. A unit cube with zero initial temperature and the top surface maintained at a constant temperature of 100 °C for $t>0$.

Table 2
Time-temperature history at the base of a cube heated suddenly at the tope.

Time elapsed(s)	Analytic (°C)	Numerical solutions of LT-BFM		Numerical solution in [24], $\Delta t=0.2$
		$N=4$	$N=6$	
0.8	5.07	5.13817	5.07063	4.34
1.6	22.77	22.7761	22.7644	21.90
2.4	39.32	39.2683	39.3288	38.86
3.2	52.55	52.5178	52.5569	52.46
4.0	62.92	62.9096	62.9276	63.05
4.8	71.03	71.0099	71.0331	71.26
5.6	77.36	77.2926	77.3642	77.64
6.4	82.31	82.0853	82.3113	82.58
7.2	86.18	84.8789	86.1775	86.40
8.0	89.20	90.0381	89.1989	89.37
8.8	91.56	91.9454	91.5601	91.68
9.6	93.41	93.6681	93.4054	93.47

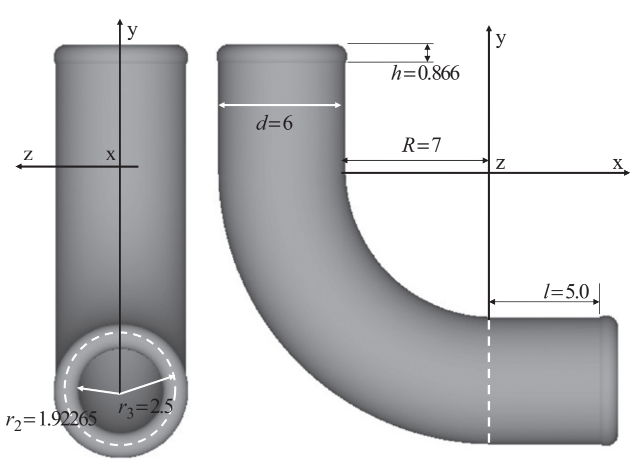

Fig. 2. An elbow pipe and its main dimensions.

maintained for $t>0$ like in Fig. 1. All the other faces are thermally insulated. The thermal diffusive a is $0.125\ \mathrm{m^2/s}$. The time-temperature history is studied at the base of the cube. In our application, 150 boundary linear triangle elements with 576 nodes are employed. We compare the results with the analytical solution in Table 2.

In Table 2 we can find that numerical solutions with our method are accurate. N is the parameter in Laplace inversion which is the same as in Eq. (48). The number of significant digits is about equal to 3 when $N=4$ and is about equal to 4 when $N=6$. There are four more equations to be solved when $N=6$ than $N=4$ in LS. Compared with the poor accuracy of early phase in most of the time domain approach, the results provided by our method is quite accurate even in early steps.

Example 2. Heat conduction on an elbow pipe

In this example, an elbow pipe with its geometry and dimensions listed in Fig. 2 is considered.

The following analytical field is used:

$$u(X,t)=x^4+12y^2+12z+12x^2t+12t^2+24t \tag{52}$$

the thermal diffusivity is $a=1\ \mathrm{m^2/s}$. The initial temperature for this problem is given by:

$$u_0=x^4+12y^2+12z \tag{53}$$

The initial temperature distribution is expressed by a polynomial function, thus the domain integral can be analytically converted to boundary integrals when $M>3$ as introduced before. In LS, the Neumann boundary condition is given as follows:

$$\bar{q}(X,s)=\left(\frac{4x^3}{s}+\frac{24x}{s^2},\ \ \frac{24y}{s},\ \ \frac{12}{s}\right)\times\vec{n}(x,y,z) \tag{54}$$

In this analysis, 332 elements and 1252 nodes are used. N is equal to 4. Fig. 3 and Fig. 4 show the numerical solutions of temperature and flux, respectively, which are compared with the exact solutions. The view points in the domain are distributed along the circle, whose coordinate $y=0$ (have been shown in Fig. 2) and the radius of which is Section 2.5. The angle between the neighbor points is 15°.

The numerical solutions show that the heat conduction problem with non-uniform polynomial distributed initial temperature can be accurately solved by our method.

Example 3. A cube with heat generation

As the last example, we analyze a cube with a heat generation. The length of the cube is $L=1$ m. It is assumed that the thermal diffusivity a is $1.6\times10^{-5}\ \mathrm{m^2/s}$. In this analysis, 150 boundary elements and 576 boundary nodes have been used. The surface

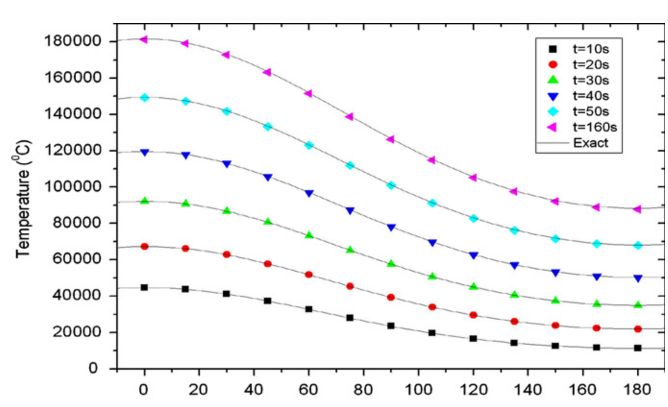

Fig. 3. Temperature distributions along the ring ($y=0$) of an elbow pipe.

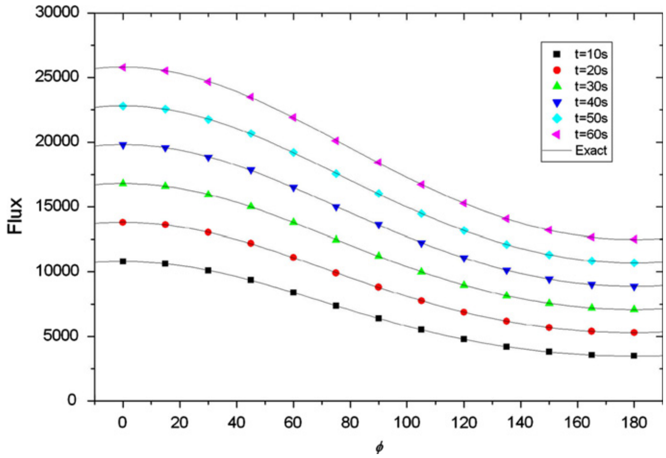

Fig. 4. Flux distributions along the ring ($y=0$) of an elbow pipe.

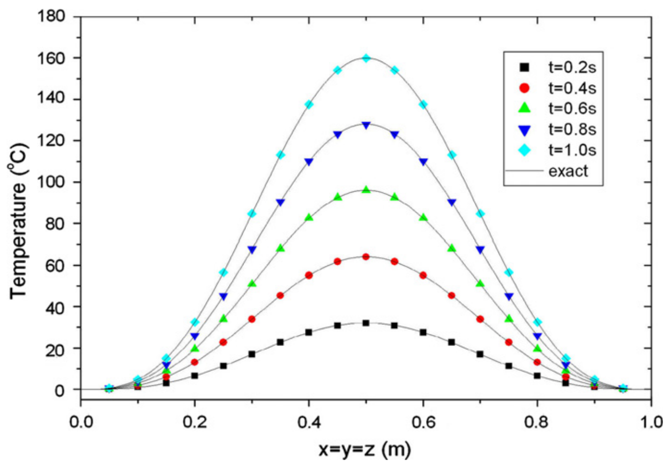

Fig. 5. Temperature distributions in cube ($x=y=z$).

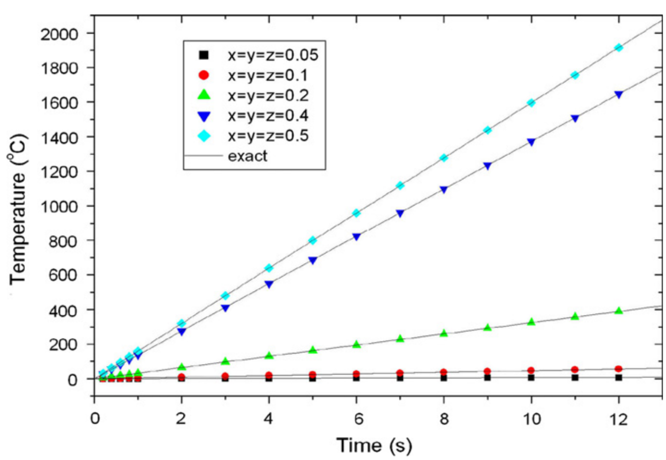

Fig. 6. Temperature variation history on several points in cube $M=3$, $N=4$.

temperature is 0 °C when $t=0$. Step heating is assumed. The heat generation is given by

$$w(x,y,z) = w_0 \sin\frac{\pi x}{L}\sin\frac{\pi y}{L}\sin\frac{\pi z}{L} \quad (t \ge 0) \tag{55}$$

The higher order form of the heat generation in MRM is

$$w^j(x,y,z) = (3\pi^2)^j \times w(x,y,z) \tag{56}$$

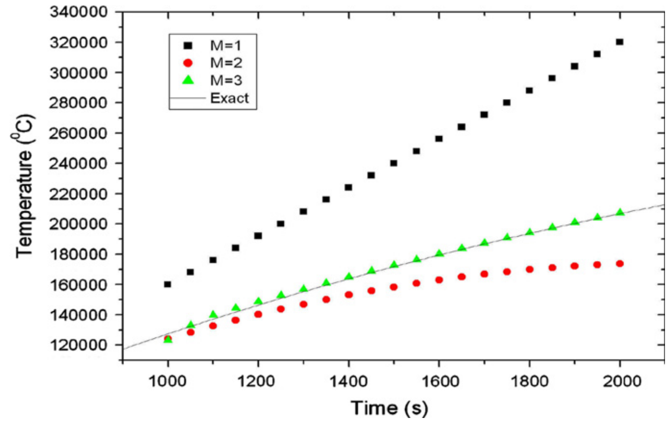

Fig. 7. Temperature variation history on point (0.5, 0.5, 0.5), $M=1$, 2, 3, and $N=4$.

This is a typical example that the coefficient of the higher order source term increases. The exact solution for this problem is

$$\begin{aligned} u(x,y,z) &= \tfrac{a w_0}{kE}\sin\tfrac{\pi x}{L}\sin\tfrac{\pi y}{L}\sin\tfrac{\pi z}{L}[1-\exp(-Et)] \\ E &= \tfrac{3a\pi^2}{L^2} \end{aligned} \tag{57}$$

where $w_0/E = 1.0\times10^5\ \mathrm{K/m^2}$ is assumed. Fig. 5 shows the comparison between the numerical solution and exact solution at $t=0.2$, 0.4, 0.6, 0.8 and 1.0 s. 19 points along the diagonal of the cube are selected as the view points in this example. Fig. 6 shows the time evolution of the temperature at points $x=y=z=0.05$, 0.1, 0.2, 0.4 and 0.5. Fig. 7 show the numerical solutions with $M=1$, 2 and 3, which are compared with the exact solution.

In this example the problem with arbitrary heat generation is solved by our method. The temperature along the diagonal of the cube is shown Fig. 5 and Fig. 6. Fig. 7 show the convergence of MRM at $t=1000$ s. Even if the higher order heat generation increases nearly 30 times of the coefficient, we only apply three terms to compute the series in Eq. (37) at $t=1000$ s.

4. Conclusion

Three-Dimension transient heat conduction problems with uniform, non-uniform initial temperature distribution and arbitrary heat generation function are solved in the paper using BEM. Numerical results illustrated the validity and accuracy of the proposed method.

In our method, with the quickly convergent higher order fundamental solutions, most of the domain integrals, which appear in the BIE of transient heat conduction problem, can be converted to several boundary integrals and non-integral terms. Furthermore, due to the simple form of the higher order fundamental solutions in our method, the implementation of our method is very simple and no additional matrix is required even for a large number of orders of the fundamental solutions.

With the help of the Gaver-Wynn-rho formulation, we computed the inverse Laplace transformation accurately and efficiently in our implementation.

Acknowledgements

This work was supported in part by National Science Foundation of China under grant numbers 10972074 and 11172098, and in part by National 973 Project of China under grant number 2010CB328005.

References

[1] Brebbia CA, Telles JCF, Wrobel LC. Boundary element techniques—theory and applications in engineering. Berlin: Springer; 1984 47–107.
[2] Rizzo FJ, Shippy DJ. A method of solution for certain problems of transient heat conduction. AIAA J 1970;8(11):2004–9.
[3] Chang Y, Kang C, et al. The use of fundamental Green's functions for the solution of problems of heat conduction in anisotropic media. Int J Heat Mass Transfer 1973;16(10):1905–18.
[4] Ochiai Y, Kitayama Y. Three-dimensional unsteady heat conduction analysis by triple-reciprocity boundary element method. Eng Anal Boundary Elem 2009;33(6):789–95.
[5] Tanaka M, Matsumoto T, et al. Dual reciprocity BEM based on time-stepping scheme for the solution of transient heat conduction problems. Int Ser Adv Boundary Elem 2002:299–308.
[6] Nowak AJ, Neves AC. The multiple reciprocity boundary element method. Springer; 1994 45–67.
[7] Nowak AJ. Application of the multiple reciprocity BEM to nonlinear potential problems. Eng Anal Boundary Elem 1995;16(4):323–32.
[8] Chen JT, Wong FC. Dual formulation of multiple reciprocity method for the acoustic mode of a cavity with a thin partition. J Sound Vib 1998;217(1):75–95.
[9] Yeih W, Chen J, et al. A study on the multiple reciprocity method and complex-valued formulation for the Helmholtz equation. Adv Eng Software 1998;29(1):1–6.
[10] Zhang J, Qin X, et al. A boundary face method for potential problems in three dimensions. Int J Numer Methods Eng 2009;80(3):320–37.
[11] Qin XY, Zhang J, et al. A finite element implementation of the boundary face method for potential problems in three dimensions. Eng Anal Boundary Elem 2010;34:934–43.
[12] Zhou F, Zhang J, et al. Shape variable radial basis function and its application in dual reciprocity boundary face method. Eng Anal Boundary Elem 2011;35(2):244–52.
[13] Zhou F, Zhang J, et al. A dual reciprocity boundary face method for 3D non-homogeneous elasticity problems. Eng Anal Boundary Elem 2012;36(9):1301–10.
[14] Dubner H, Abate J. Numerical inversion of Laplace transforms by relating them to the finite Fourier cosine transform. J ACM (JACM) 1968;15(1):115–23.
[15] Hassanzadeh H, Pooladi-Darvish M. Comparison of different numerical Laplace inversion methods for engineering applications. Appl Math Comput 2007;189(2):1966–81.
[16] Talbot A. The accurate numerical inversion of Laplace transforms. IMA J Appl Math 1979;23(1):97.
[17] Abate J, Valkó P. Multi-precision Laplace transform inversion. Int J Numer Methods Eng 2004;60(5):979–93.
[18] Weideman J, Trefethen L. Parabolic and hyperbolic contours for computing the Bromwich integral. Math Comput 2007;76(259):1341.
[19] Abate J, Choudhury GL, et al. On the Laguerre method for numerically inverting Laplace transforms. INFORMS J Comput 1996;8:413–27.
[20] Gaver Jr DP. Observing stochastic processes, and approximate transform inversion. Oper Res 1966:444–59.
[21] Valko PP, Abate J. Comparison of sequence accelerators for the Gaver method of numerical Laplace transform inversion. Comput Math Appl 2004;48(3–4):629–36.
[22] Kano PO, Brio M. Application of post's formula to optical pulse propagation in dispersive media. ComputMath Appl 2010;59(2):629–50.
[23] 〈http://en.wikipedia.org/wiki/Thermal_diffusivity〉.
[24] Gupta A, Sullivan Jr JM, et al. An efficient bem solution for three-dimensional transient heat conduction. Int J Numer Methods Heat Fluid Flow 1995;5(4):327–40.